Dynamics of a simplified p53 Boolean network

Bradley Karas
Arizona State University
(Dated: April 28, 2016)

The p53 tumor suppressor gene has been shown to be involved in the prevention of cancer and aging of other animals. It has been the target of much research as the network that controls it holds opportunities for possible anti-cancer and anti-aging therapies. A simplified version of the p53 network was analyzed as a Boolean network. The dynamics of the system both in the presence and absence of DNA damage were analyzed. Measurements of the active information and transfer entropy of the nodes and links were obtained.

I. INTRODUCTION

Tens of thousands of damaging events occur in every cell on a daily basis (Lindahl and Nyberg 1972). DNA damage triggers cellular responses through highly conserved DNA damage checkpoint mechanisms that arrest cell cycle progression or evokes cellular senescence and apoptosis (Jackson and Bartek 2009). This is actually a good thing as cellular senescence and apoptosis has been shown to be a barrier to the formation of tumors (Bartkova *et al.* 2005). The tumor suppressor p53 has been shown to be one of these checkpoint mechanisms that controls cell fate in response to DNA damage (Purvis *et al.* 2012). In the presence of DNA damage from either aging or cancer development, p53 causes the cell to undergo cell cycle arrest, senescence, or apoptosis depending on the severity of DNA damage (Reinhardt and Schumacher 2012). In approximately 50% of human cancers, p53 has been found to have been inactivated (Petitjean *et al.* 2007). Thus, the inhibition or enhancement of target genes or pathways in the p53 network have been targeted as prospective anti-cancer therapies in several types of cancer (Hussain *et al.* 2015). Understanding the dynamics of the p53 gene regulatory network is thus important to understanding how cancer aging affect our cells and the types of therapies that might be available to counteract that damage to our cells.

II. MODEL DESCRIPTION

The simplified p53 network was defined by (Choi *et al.* 2012) that included 16 nodes with 50 links. The network can be seen in Figure 1. The simplified network was modeled as a Boolean network. The nodes were treated as being either "On" and active or "Off" and inactive at each time step. The state of a node at each time step was calculated using Equation 1 where $S_i(t)$ is the state of the node i at time t, a_{ij} is the weight of the interaction between the target node i and linked node j, and b_i is the base value of the node in the absence of input(Choi *et al.* 2012). The table of Boolean rules specifying the state transition logic can be found in Table S1 in the supplement.

$$S_i(t+1) = \begin{bmatrix} 1, & if & b_i + (\sum_j a_{ij} S_j(t)) > 0 \\ 0, & elseif & b_i + (\sum_j a_{ij} S_j(t)) < 0 \\ S_i(t), & elseif & b_i + (\sum_j a_{ij} S_j(t)) = 0 \end{bmatrix} \quad (1)$$

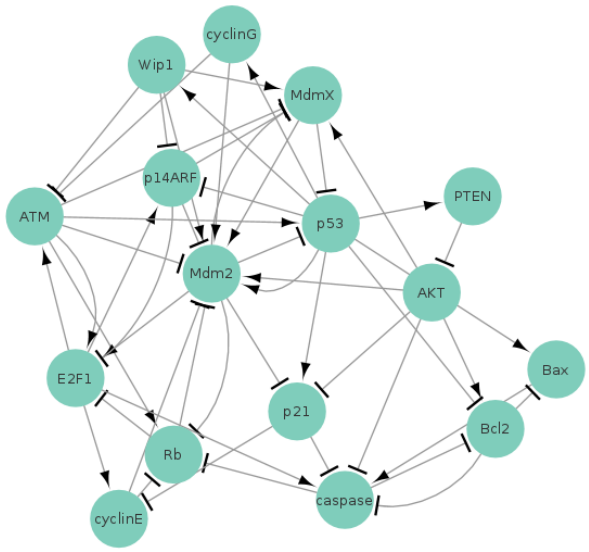

FIG. 1. Simplified p53 network. Arrows indicate activating links and perpendicular bars indicate inhibitory processes.

III. RESULTS

Two versions of the p53 network were analyzed and compared. The first version, "Normal 0", was the p53 network for the normal cell without the presence of DNA damage. The attractor landscape can be seen in Figure 2, which consisted of a single point attractor. The maximum path length to the attractor was 10 with a characteristic path length of 3.39. The second version, "Normal 1", was the p53 network for the normal cell with the presence of DNA damage without the deletion of any nodes or links. The attractor landscape for the "Normal 1" had a single cyclic attractor and can be seen in Figure 3.

The maximum path length to the attractor was 10 with a characteristic path length of 6.18. The stable states for both can be seen in Table I.

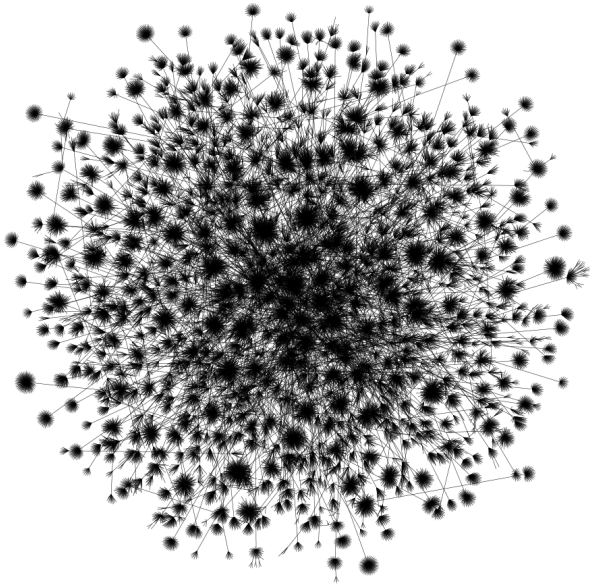

FIG. 2. Attractor landscape for 0 normal.

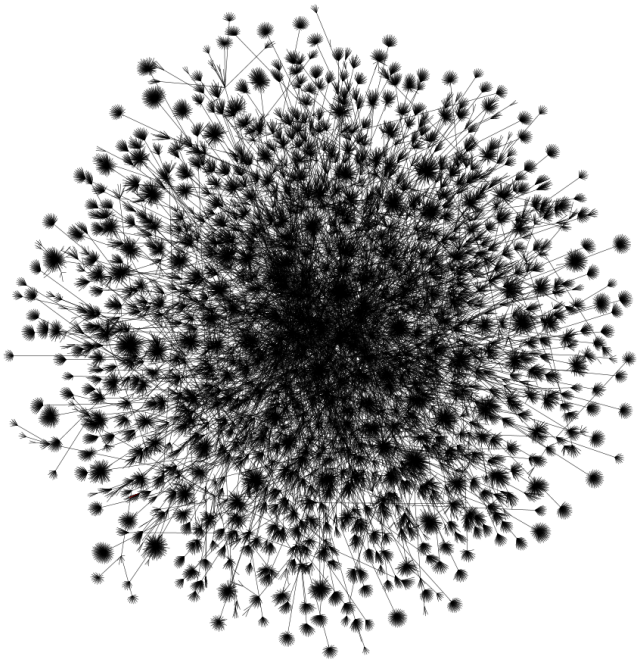

FIG. 3. Attractor landscape for 0 normal.

The active information of both versions of the network was measured over a range of history lengths and maximum step sizes. Figure 4 and Figure 5 both show the active information measured over the same maximum step size of 10 for a range of history lengths for the absence and presence of DNA damage respectively. Additional plots of active information can be found in the supplement.

TABLE I. Stable states of the p53 network in the presence or absence of DNA damage as represented by "1" or "0" respectively in column 1.

DNA damage condition	Type	ATM	p53	Mdm2	MdmX	Wip1	cyclinG	PTEN	p21	AKT	cyclinE	Rb	E2F1	p14ARF	Bcl-2	Bax	caspase
0_Normal	Point	0	0	1	0	0	0	0	0	1	1	0	1	0	1	0	0
1_Normal	Cyclic	1	0	0	0	0	0	0	0	1	1	0	1	1	0	0	0
		1	1	0	0	0	0	0	0	1	1	1	0	1	1	0	0
		1	1	0	0	1	1	1	1	0	0	1	0	0	1	0	0
		0	0	0	1	1	1	1	1	0	0	1	1	0	0	0	0
		0	0	1	0	0	0	0	0	0	0	0	1	0	0	0	0

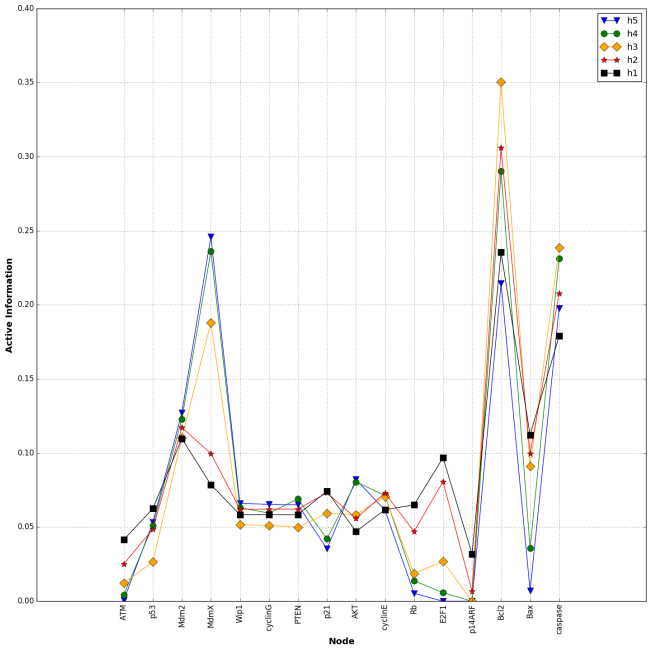

FIG. 4. Active information for "0 Normal" at history lengths of 1, 2, 3, 4 and 5 with a step size of 10.

The transfer entropy was measured for both versions of the network over a range of maximum step sizes and history lengths. The transfer entropy measured was then scaled in each case from greatest to smallest transfer entropy for each link. Figure 6 and Figure 7 both show the transfer entropy measured over a maximum step size of 10 for a range of history lengths for the absence and presence of DNA damage respectively. Figure 8 shows the transfer entropy plotted against the active information for maximum step size of 10 and history length of 1. Additional plots of transfer entropy can be found in the supplement.

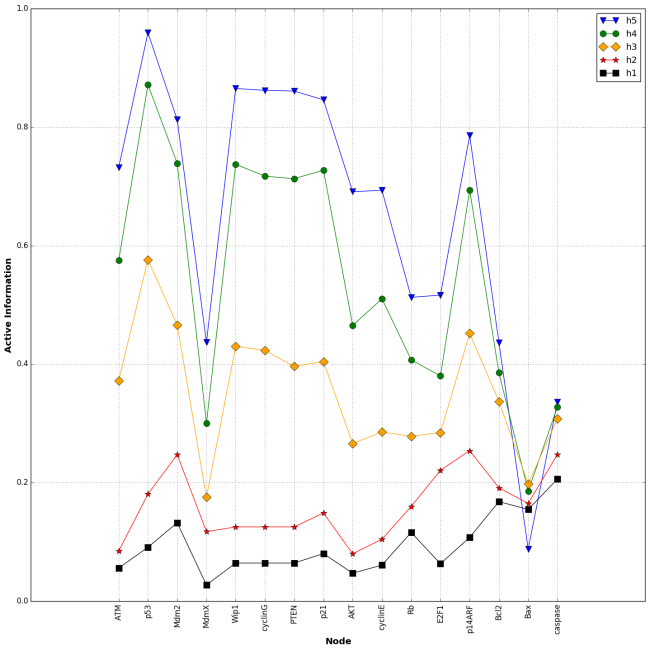

FIG. 5. Active information for "1 Normal" at history lengths of 1, 2, 3, 4 and 5 with a step size of 10.

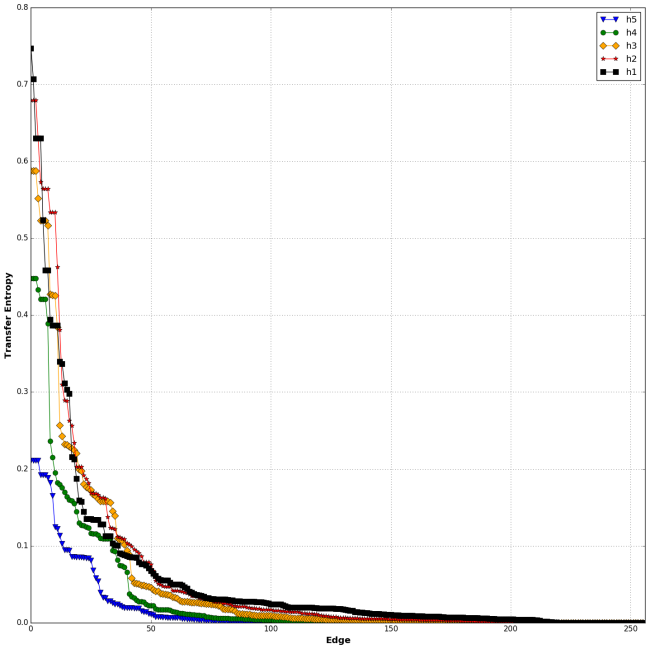

FIG. 6. Transfer entropy for "0 Normal" at history lengths of 1, 2, 3, 4 and 5 with a step size of 10.

IV. SUMMARY/DISCUSSION

Both networks had a single basin for all 65,536 possible initial states. It was quite interesting to note that the two versions of the simplified p53 network have the same topology, but quite different dynamics due to having different base values (b_i) in the presence and absence of DNA damage. [floatfix] For the network that has DNA damage present, active information increases as history length increases with the exception of Bax. This was somewhat expected for the majority of nodes other than Bax as this network had a cyclic attractor and the characteristic path length is only 6.18. This would imply more information would be stored by each node as the history length increases. When the state of the network enters the cyclic attractor there are only 7 possible states for the network to be in. Why Bax would be different in this case is not clear. Conversely, one would expect there to be less information stored in each node for the network that consists of a single point attractor with little correlation to history length. This was exactly what was measured. [floatfix] The transfer entropy in both networks decreased predictably as the history length was increased. It was interesting to note that both networks have plateaus in their scaled transfer entropy. The heat maps of transfer energy in both networks showed similar structures as seen in Figure 8. In both networks, AKT and cyclin E had a high amount of transfer entropy to their respective nodes by p21, PTEN, cyclin G and Wip 1. This may have been because they are both involved in the regulation of the cell cycle. Also of note was that in the presence of DNA damage ATM was a high transfer entropy destination node for p21, PTEN, cyclin G, and Wip1. Those same source nodes were destination nodes for p53. The p21, PTEN, cyclin G, and Wip1 nodes formed feedback loops with p53 and ATM. Thus, we can

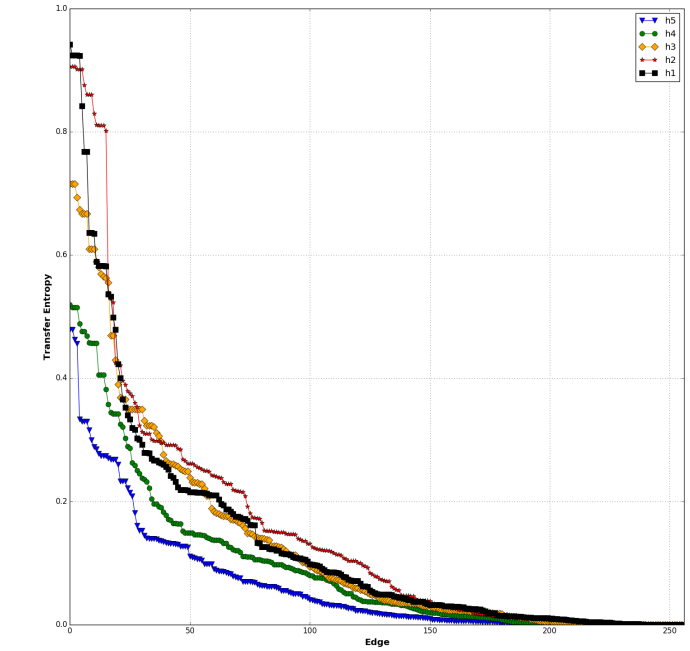

FIG. 7. Transfer entropy for "1 Normal" at history lengths of 1, 2, 3, 4 and 5 with a step size of 10.

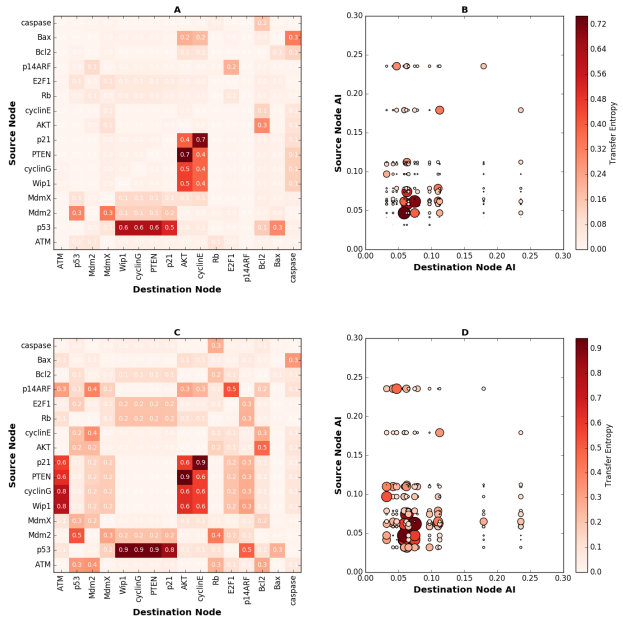

FIG. 8. Transfer entropy heat maps for history length of 1 and maximum step size of 10. In each subplot, the source node for interactions is on the x-axis and the destination node is on the y-axis. The temperatures for all of the subplots are the transfer entropy values. (A) and (B) are heat maps for the "0 Normal" network. (C) and (D) are heat maps for the "1 Normal" network. (B) and (D) are the same heat maps for (A) and (C) respectively, but the x and y axes are the values for the active information at the source and destination nodes. The size of the bubbles for (B) and (D) are scaled to the transfer entropy values.

see from the transfer of information that the presence of DNA damage indicated by the activation of ATM triggers feedback loops associated with p53. This further validates the supposition that p53 is involved with the cellular response to DNA damage, especially given that the same feedback loops were not activated by ATM when there was no damage present. [floatfix] The dynamics of the simplified system are intriguing and warrant further study. In particular, the dynamics of the system having undergone single node or single link deletions due to DNA damage is needed. This would give insight into how robust the p53 network is to actual DNA damage. This may yield information as to which nodes and links, when deleted, alter the fate of the cell such that the cell enters apoptosis rather than cell cycle arrest. Being able to target specific nodes or links based on DNA damage could yield possible tailored anti-cancer drugs that would force the damaged cells to under go apoptosis while leaving the healthy cells alone. [floatfix]

Bartkova, J., Z. Hořejší, K. Koed, A. Krämer, F. Tort, K. Zieger, P. Guldberg, M. Sehested, J. M. Nesland, C. Lukas, *et al.*, 2005, Nature **434**(7035), 864.
Choi, M., J. Shi, S. H. Jung, X. Chen, and K.-H. Cho, 2012, Sci. Signal. **5**(251), ra83.
Hussain, M., K. Tian, L. Mutti, M. Krstic-Demonacos, and J.-M. Schwartz, 2015, Genomics and Computational Biology **1**(1), 20.
Jackson, S. P., and J. Bartek, 2009, Nature **461**(7267), 1071.
Lindahl, T., and B. Nyberg, 1972, Biochemistry **11**(19), 3610.
Petitjean, A., E. Mathe, S. Kato, C. Ishioka, S. V. Tavtigian, P. Hainaut, and M. Olivier, 2007, Human mutation **28**(6), 622.
Purvis, J. E., K. W. Karhohs, C. Mock, E. Batchelor, A. Loewer, and G. Lahav, 2012, Science **336**(6087), 1440.
Reinhardt, H. C., and B. Schumacher, 2012, Trends in Genetics **28**(3), 128.